TRIP13 overexpression promotes gefitinib resistance in non-small cell lung cancer via regulating autophagy and phosphorylation of the EGFR signaling pathway

ZHANGXIAN XIAO[1], MINGXI LI[1], XIAOQIAN ZHANG[1], XUEZHU RONG[2*] and HONGTAO XU[1*]

[1]Department of Pathology, The First Hospital and College of Basic Medical Sciences, China Medical University, Shenyang, Liaoning 110122; [2]Department of Pathology, The First Hospital of China Medical University, Heping, Shenyang, Liaoning 110001, P.R. China

Received September 20, 2022; Accepted February 16, 2023

DOI: 10.3892/or.2023.8521

Abstract. Non-small cell lung cancer (NSCLC) accounts for the majority of lung cancers and remains the most common cause of cancer-related death. Epidermal growth factor receptor (EGFR) tyrosine kinase inhibitors (EGFR-TKIs) have been used as first-line treatment for patients with NSCLC showing *EGFR* mutations. Unfortunately, drug resistance is a crucial barrier affecting the treatment of patients with NSCLC. Thyroid hormone receptor interactor 13 (TRIP13) is an ATPase that is overexpressed in numerous tumors and is involved in drug resistance. However, whether TRIP13 plays a role in regulating sensitivity to EGFR-TKIs in NSCLC remains unknown. TRIP13 expression was evaluated in gefitinib-sensitive (HCC827) and -resistant (HCC827GR and H1975) cell lines. The effect of TRIP13 on gefitinib sensitivity was assessed using the MTS assay. The expression of TRIP13 was upregulated or knocked down to determine its effect on cell growth, colony formation, apoptosis and autophagy. Additionally, the regulatory mechanism of TRIP13 on EGFR and its downstream pathways in NSCLC cells were examined using western blotting, immunofluorescence and co-immunoprecipitation assays. The expression levels of TRIP13 were significantly higher in gefitinib-resistant than in gefitinib-sensitive NSCLC cells. TRIP13 upregulation enhanced cell proliferation and colony formation while reducing the apoptosis of gefitinib-resistant NSCLC cells, suggesting that TRIP13 may facilitate gefitinib resistance in NSCLC cells. In addition, TRIP13 improved autophagy to desensitize gefitinib in NSCLC cells. Furthermore, TRIP13 interacted with EGFR and induced its phosphorylation and downstream pathways in NSCLC cells. The present study demonstrated that TRIP13 overexpression promotes gefitinib resistance in NSCLC by regulating autophagy and activating the EGFR signaling pathway. Thus, TRIP13 could be used as a biomarker and therapeutic target for gefitinib resistance in NSCLC.

Correspondence to: Professor Hongtao Xu, Department of Pathology, The First Hospital and College of Basic Medical Sciences, China Medical University, 77 Puhe Road, Shenyang North New Area, Shenyang, Liaoning 110122, P.R. China
E-mail: xuht@cmu.edu.cn

Professor Xuezhu Rong, Department of Pathology, The First Hospital of China Medical University, 155 Nanjing North Street, Heping, Shenyang, Liaoning 110001, P.R. China
E-mail: rxz-168@163.com

*Contributed equally

Abbreviations: NSCLC, non-small cell lung cancer; EGFR, epidermal growth factor receptor; EGFR-TKIs, epidermal growth factor receptor tyrosine kinase inhibitors; TRIP13, thyroid hormone receptor interactor 13; LUAD, lung adenocarcinoma; LUSC, lung squamous cell carcinoma; IC_{50}, half-maximal inhibitory concentration

Key words: TRIP13, EGFR, gefitinib resistance, autophagy, NSCLC

Introduction

Lung cancer is the leading cause of cancer-related deaths worldwide and remains one of the most recalcitrant tumors, with a poor five-year survival rate. More than 85% of the lung cancers are non-small cell lung cancers (NSCLCs), mainly composed of lung adenocarcinoma (LUAD) and lung squamous cell carcinoma (LUSC) (1). In an Asian population, over half of the patients with NSCLC carry epidermal growth factor receptor (*EGFR*) 19 del (54%) or 21 L858R (43%) mutations, leading to the recommendations to use EGFR tyrosine kinase inhibitors (EGFR-TKIs) (2). Clinically, EGFR-TKIs, such as gefitinib, are still used as first-line antitumor drugs for patients with NSCLC showing mutations in the *EGFR*. According to current evidence, EGFR-TKIs can improve not only the objective response rate, but also the progression-free survival rate of affected patients. However, ~six months to a year after using EGFR-TKIs, the tumor acquires drug resistance, greatly minimizing the clinical benefit to patients with NSCLC. Notably, T790M mutations in *EGFR* induce first- and second-generation TKI resistance in more than half

of the NSCLC cases. In addition, ~30% of the resistance cases remain unelucidated (3,4). Hence, overcoming resistance to EGFR-TKIs has become imperative for the development of NSCLC-targeted treatment.

Thyroid hormone receptor interactor protein 13 (TRIP13, also known as pachytene checkpoint 2), one of the most important members of the AAA^+ ATPase family, plays important roles in cell cycle checkpoints, DNA repair, meiotic recombination and chromosome synapsis (5-10). Accumulating evidence suggests that TRIP13 is overexpressed in several human malignancies and is closely associated with poor prognosis in various diseases, including colorectal cancer, hepatocellular carcinoma, prostate cancer, glioblastoma, thyroid cancer and ovarian cancer (11-16). Regarding the role of TRIP13 in lung cancer, previous research has focused on its activation of the PI3K/AKT/mTOR signaling pathway (17,18). A recent study by the authors showed that TRIP13 could promote lung cancer development by activating the epithelial-mesenchymal transition and Wnt signaling pathways (19). Notably, as demonstrated in previous studies, TRIP13 activation also facilitates chemotherapy resistance in bladder cancer and multiple myeloma as well as radiation resistance in head and neck cancer (20-22). However, the role of TRIP13 in the modulation of EGFR-TKIs sensitivity in NSCLC remains unclear.

Cell autophagy is a catabolic process that is required to maintain cell homeostasis. Previous research has shown that it is associated with several biological processes, including cell differentiation, development and survival (23-25). Although the role of autophagy in cell death and survival has not been thoroughly established, it has been demonstrated that autophagy is boosted in cancer cells when they are subjected to harsh conditions, such as anticancer medication therapy, which may lead to anticancer drug resistance (26-28).

The EGFR signaling pathway is often dysregulated in various human cancers (29,30). When EGFR binds to a ligand, it becomes phosphorylated, thereby activating its downstream signaling pathways. As a result, anti-apoptotic and pro-survival processes are triggered in cancer cells to promote tumor progression. Therefore, patients with *EGFR* mutations could greatly benefit from EGFR-TKIs, such as gefitinib or erlotinib, which block the action of this pathway (31,32).

In the present study, resistance to gefitinib and pro-cancer effects of TRIP13 in NSCLC were identified. The effects of TRIP13 on autophagy and phosphorylation of the EGFR signaling pathway were also explored by regulating the expression of TRIP13 in gefitinib-sensitive and -resistant NSCLC cells. Taken together, the present results suggested that the downregulation of TRIP13 improves the sensitivity of NSCLC cells to gefitinib. TRIP13 expression has the potential to serve as a gefitinib-resistant biomarker for NSCLC.

Materials and methods

Patients and specimens. A total of 160 NSCLCs and 19 corresponding normal lung tissue samples were collected from 160 patients (age and sex distribution are presented in Table I) who underwent complete surgical excision of LUAD or LUSC at the First Affiliated Hospital of China Medical University between May 2018 and August 2020. All tissue specimens were fixed in 4% neutral formaldehyde at room temperature for 24 h, embedded in paraffin, and sectioned into 4-μm slices. In addition, a total of 20 pairs of fresh NSCLC tissue samples and the corresponding normal lung tissue samples were collected and stored at -80˚C immediately after resection. Neither chemotherapy nor neoadjuvant radiotherapy was performed before the surgery. The World Health Organization classification of lung tumors (4th edition, 2015) was used to evaluate histological diagnosis and grade. The eighth edition of the American Joint Committee on Cancer (AJCC) lung cancer staging system was used for tumor staging. The present study was approved [approval no. LS (2021)009] by the Research Ethics Committee of the China Medical University (Shenyang, China). Written informed consent was obtained from all patients.

Bioinformatics analysis. The Kaplan-Meier plotter (http://kmplot.com/analysis/) was used to generate overall survival curves (examined by the log-rank test) for patients with lung cancer showing high or low TRIP13 expression. TRIP13 expression in patients with LUAD and LUSC at various cancer stages was collected from the Cancer Genome Atlas database (TCGA; http://cancergenome.nih.gov/). Gene Expression Profiling Interactive Analysis (GEPIA; http://gepia.cancer-pku.cn/) was used to perform a correlation analysis between TRIP13 and EGFR expression in lung cancers.

Cell culture and transfection. Human lung cancer cell lines HCC827 (with *EGFR* 19del) and H1975 (with *EGFR* L858R and T790M mutations) were obtained from the Shanghai Cell Bank. Gefitinib sensitivity is linked to *EGFR* E746-A750 deletion in exon 19 of the HCC827 cell line. The H1975 cell line carried an *EGFR* T790M mutation in exon 20, which is related to gefitinib resistance.

At 37˚C in a 5% CO_2 atmosphere, cells were cultured in the RPMI-1640 medium with 10% fetal bovine serum and passaged in sterile culture dishes with 0.25% trypsin (all from Gibco; Thermo Fisher Scientific, Inc.). The gefitinib-acquired resistance cell line, HCC827GR, was established via a stepwise increase in the dosage of gefitinib (0.01, 0.1, 1, 5, 10, 20 and 40 μM). After 24 h, the gefitinib-containing medium was replaced with a regular medium. Each dose was repeated twice until the half-maximal inhibitory concentration (IC_{50}) of the HCC827GR cells was satisfactory. To sustain resistance, HCC827GR cells were cultured in a medium containing 100 nM gefitinib.

Plasmid transfection was performed using Lipofectamine® 3000 (Invitrogen; Thermo Fisher Scientific, Inc.), according to the manufacturer's instructions. Subsequent experiments were performed 24 h after plasmid transfection. The pCMV6-TRIP13 and pCMV6 plasmids were purchased from Origene Technologies, Inc Co. The plasmid containing the short hairpin RNA of small interfering RNA of TRIP13 (shTRIP13) and its negative control plasmid (shNC) were purchased from Shanghai GeneChem Co., Ltd. 600 μg/ml G418 (Sigma-Aldrich; Merck KGaA) was used to screen for stably transfected cells. The TRIP13 shRNA sequences were as follows: shTRIP13-1, 5'-CGATTATGTGATGACAACTTT-3'; shTRIP13-2, 5'-GUACCGAUAUGGCCAAUUA-3'; shTRIP13-3: 5'-GCAAAUCACUGGGUUCUAC-3'; and shCtrl: 5'-TTCTCCGAACGTGTCACGT-3'.

Table I. Correlations between TRIP13 expression and clinicopathological factors in NSCLC.

Clinicopathological factors	Total number	TRIP13-negative	TRIP13-positive	P-value
Tissue				<0.01
Normal	19	17	2	
NSCLC	160	45	115	
Pathology type				0.386
LUSC	80	21	59	
LUAD	80	26	54	
Age				0.318
<60	89	29	60	
≥60	71	18	53	
Sex				0.417
Male	119	37	82	
Female	41	10	31	
TNM Stage				<0.01
I + II	127	89	38	
II + IV	27	9	18	
Tumor status				0.825
T1 + T2	120	36	84	
T3 + T4	30	10	20	
Lymph node metastasis				<0.01
No	59	41	18	
Yes	79	25	54	
Distant metastasis				0.838
No	149	45	104	
Yes	11	3	8	

NSCLC, non-small cell lung cancer; TRIP13, thyroid hormone receptor interactor 13; LUAD, lung adenocarcinoma; LUSC, lung squamous cell carcinoma.

Gefitinib, an autophagy activator, and EGFR inhibitor, and the autophagy inhibitor, 3-methyladenin (3-MA) were purchased from MedChemExpress. Dimethyl sulfoxide (DMSO; Beijing Solarbio Science & Technology Co., Ltd.) was added for comparison.

Immunohistochemistry. Briefly, 4-μm thick tissue sections were deparaffinized in xylene, rehydrated using a gradient alcohol series, and then autoclaved for 2 min in 0.01 M citrate buffer (pH 6.0). Hydrogen peroxide (0.3%) was used to inhibit endogenous peroxidase activity, and 5% normal goat serum (Maxin Biotechnology Co., Ltd.) was added to the mixture to block non-specific binding at 37˚C for 30 min. Next, the tissue sections were incubated with a rabbit polyclonal anti-TRIP13 antibody at 4˚C for 12 h. The TRIP13 staining intensity was graded as follows: 0, no staining; 1, weak; 2, moderate; and 3, high. The percentage score classifications were 1 (1-25%), 2 (26-50%), 3 (51-75%) and 4 (76-100%). Each tumor sample received a score that was multiplied to generate a final score ranging from 0 to 12. A cut-off value of 6 was used to divide patients into positive and negative TRIP13 expression groups. Tumor samples with scores ≥6 were considered to be positive for TRIP13, whereas those with scores ≥0 and <6 were considered to be negative for TRIP13.

Western blot analysis. First, the Bradford method was used to quantify the total protein isolated from cells using cell lysis buffer (33). Sodium dimethyl sulfoxide polyacrylamide gel electrophoresis was used to separate 60 μg of protein, and the concentration (8-12%) of the gels varied with the molecular weight of the proteins. Next, the proteins were transferred to a polyvinylidene fluoride membrane (Millipore Sigma) blocked with 5% non-fat milk at 37˚C for 2 h, and incubated with primary antibodies overnight at 4˚C. The primary antibodies used in the present study are listed in Table SI. Subsequently, the membranes were then treated for 2 h at 37˚C with horseradish peroxidase-conjugated mouse (cat. no. B900620) or rabbit IgG (cat. no. 30000-0-AP) (both 1:1,000; ProteinTech Group, Inc.). Finally, the protein bands were visualized using an electrochemiluminescence substrate (Pierce; Thermo Fisher Scientific, Inc.) and detected using a bioimaging system (version 5.2.1; DNR Bio-Imaging Systems Co., Ltd.). GAPDH (1:1,000; cat. no. 600041Ig; ProteinTech Group, Inc.) was used as a loading control to determine the relative protein levels.

Cell proliferation assay. Cells were plated in a 96-well plate (~3,000 cells per well) for 24 h with a medium containing 10% fetal bovine serum after transfection. After switching to

serum-free medium, 3-(4,5-dimethylthiazol-2-yl)-5 -(3-carbo xymethoxyphenyl)-2-(4-sulfophenyl)-2H-tetrazolium (MTS; Dojindo Molecular Technologies, Inc.) was added to each well (20 μl/well) and incubated at 37˚C for 2 h. To construct a growth curve, data were measured spectrophotometrically every 24 h for 5 days at a wavelength of 490 nm. After seeding the cells in 96-well plates for 24 h, different concentrations of gefitinib were added and incubated for 72 h to determine the IC_{50} of gefitinib. Cell viability was assessed as aforementioned. GraphPad Prism (version 9.0; GraphPad Software, Inc.) was used to calculate the IC_{50} values.

Colony formation assay. After 24 h of transfection, the cells were cultured in six-well plates (~800 cells/well). After the cells were fully apposed, gefitinib (0.5 μM for HCC827 cells and 5 μM for H1975 and HCC827GR cells) was added, and the cells were incubated for 72 h before being replaced with normal medium. During this experiment, the culture medium was changed every 3-4 days for 10-15 days. The cells were then rinsed in phosphate-buffered saline (PBS; Gibco; Thermo Fisher Scientific, Inc.), fixed for 20 min at 37˚C with 4% paraformaldehyde, and stained for 10 min at 37˚C with Giemsa solution (Beyotime Biotechnology Inc.). Colonies with >50 cells were counted.

Cell apoptosis assay. Cells were seeded in a 6-cm culture dish, and gefitinib (0.5 μM for HCC827 cells and 5 μM for H1975 and HCC827GR cells) was added for 24 h. The cells were then cultured for another day. The cells from each tube were suspended in binding buffer (0.5 ml of binding buffer and 5 μl of Annexin V-fluorescein isothiocyanate (Annexin V-FITC) and propidium iodide were added as required (both from Shanghai GeneChem Co., Ltd.). Apoptosis was examined using flow cytometry (Accuri™ C6 Plus), and the data was analyzed using FlowJo (version 10.0; both from Becton Dickinson and Company Technology Co., Ltd.).

Tumor xenograft mouse models. A total of 14 female BALB/c nude mice (age, four weeks-old; weight, 22±1.5 g) were acquired from Charles River Laboratories (Beijing, China). The mice were kept in plastic cages (three mice/cage), with free access to food and water, and under controlled lighting (12/12 h light/dark cycle), temperature (23±2˚C) and humidity (50%). The axilla of each mouse was then subcutaneously injected with $5x10^6$ tumor cells in 0.2 ml of sterile PBS. The mice were euthanized and autopsied six weeks after inoculation to observe tumor development. All mice that reached the study's endpoint were euthanized by cervical dislocation. The humane endpoints were defined as the following: the xenograft tumor diameter was >20 mm, the xenograft tumor reached >20% of the animal body weight, a body weight loss of >20% happened due to tumor growth, and symptoms of immobility, inability to eat, ulceration, infection, or necrosis were observed. The appearance of dilated pupils, as well as the absence of breath and heartbeat, served as evidence of death. Animal experiments were approved by The Institutional Animal Research Committee of the China Medical University. The entire process complied (IACUC issue no. KT2022488) with the experimental animal ethics guidelines of China Medical University (Shenyang, China).

Laser confocal immunofluorescence assay. The NSCLC cells were cultured on coverslips in 24-well plates. After 24 h, the cells were fixed for 20 min with 4% paraformaldehyde and permeabilized for 10 min with 0.1% Triton X-100 (Beyotime Institute of Biotechnology). The slides were washed three times with PBS, blocked with bovine serum albumin (Beijing Solarbio Science & Technology Co., Ltd.) for 2 h at 25˚C, and incubated overnight at 4˚C with anti-TRIP13 (1:50; cat. no. 19602-1-AP; ProteinTech Group, Inc.), or anti-EGFR (1:50; cat. no. ab52894; Abcam). The cells were then washed again and incubated for 2 h at 25˚C with tetramethylrhodamine (TRITC; 1:50; cat. no. SA00007-1; ProteinTech Group, Inc.) or FITC-conjugated secondary antibodies (1:50; cat. no. SA00003-8; ProteinTech Group, Inc.), and cell nuclei were counterstained with DAPI (Beyotime Institute of Biotechnology) for 10 min. An Olympus FV1000 laser scanning confocal microscope (Olympus Corporation) was used for the immunofluorescence analysis.

Co-immunoprecipitation assay. Cells were lysed in a solution of NP-40 (Beyotime Biotechnology Inc.) and protease inhibitor mixture. The lysates were centrifuged at 12,000 x g at 4˚C for 20 min. The lysates were then combined and incubated overnight with protein G-agarose beads (Bimake Biotechnology Co., Ltd.) or appropriate primary antibodies at 4˚C. Western blotting was used to analyze the results.

Statistical analysis. Statistical analyses were performed using GraphPad Prism (version 9.0; GraphPad Software Inc.). All values from the studies are expressed as the mean ± standard deviation. Chi-square test and Spearman's rank correlation were used to examine the immunohistochemical results. The expression of TRIP13 in tumors and corresponding normal lung tissues from the same patients were compared using a paired t-test, while other data from two groups were compared using an unpaired t-test. Differences between three or more groups were evaluated using a one-way ANOVA multiple comparison test, followed by Tukey's post hoc test. The statistical significance of differences between groups was determined using $P<0.05$.

Results

Increased TRIP13 expression in patients with NSCLC is related to the individual cancer stages and poor prognosis. The expression of TRIP13 was examined by immunohistochemistry in 160 NSCLC and 19 normal lung specimens, which were collected from paraffin-embedded tissues. TRIP13 positive expression was seldom observed in normal alveolar cells in corresponding normal lung tissues (10.5%) but was commonly noted in the cytoplasm of 160 cases (71.8%) of NSCLC (Table I; Fig. 1A-C). Western blot analysis confirmed that the expression levels of TRIP13 were significantly higher in lung cancer tissues than in normal lung samples, both of which were collected from fresh tissues (n=20) (Fig. 1D and E). As indicated in Table I, the expression of TRIP13 was correlated with the TNM stage and lymph node metastasis of NSCLC, but was not significantly correlated with patient age, sex, tumor status or distant metastasis.

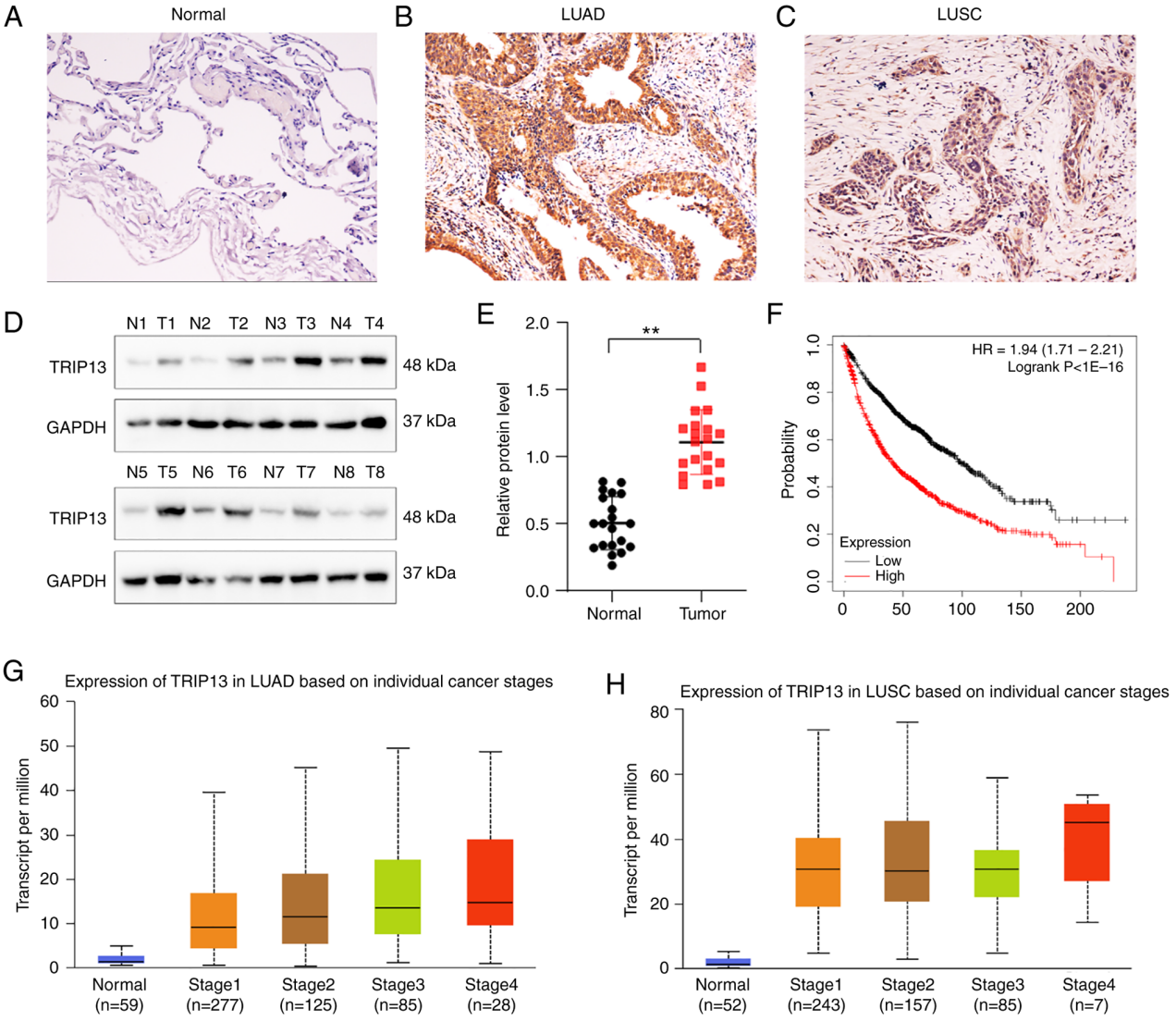

Figure 1. TRIP13 expression in patients with non-small cell lung cancer and its relation to each cancer stage and patient prognosis. (A) Immunohistochemical staining for TRIP13 in normal lung tissues and lung cancer tissues (magnification, x200). (B and C) Immunohistochemical staining for TRIP13 in LUAD and LUSC (magnification, x200). (D and E) Western blot analysis and relative expression levels of TRIP13 in lung primary tumor tissues and corresponding normal lung tissues (n=20). (F) Kaplan-Meier (KM) graphs of overall survival of patients with lung cancer from the online database KM-plotter. (G and H) Expression of TRIP13 based on each cancer stage in LUAD and LUSC from The Cancer Genome Atlas database. **P<0.01. TRIP13, thyroid hormone receptor interactor 13; LUAD, lung adenocarcinoma; LUSC, lung squamous cell carcinoma; N, corresponding normal lung tissue; T, lung primary tumor tissue; HR, hazard ratio.

Kaplan-Meier survival analysis indicated that patients with lung cancer showing higher TRIP13 levels had a poorer overall survival rate (Fig. 1F). Based on the findings from the TCGA database, TRIP13 was also overexpressed in different individual lung cancer stages (Fig. 1G and H) as well as in the histological subtypes LUADs and LUSCs (Fig. S1A and D). In addition, analyses of TCGA database revealed that TRIP13 expression was linked to nodal metastasis status and patient age (Fig. S1B, C, E, and F).

Increased expression of TRIP13 induces gefitinib resistance in NSCLC cells. HCC827 cells were used as gefitinib-sensitive NSCLC cells, and H1975 and HCC827GR cells as natural and acquired gefitinib-resistant NSCLC cells, respectively. As indicated in the MTS assays, both HCC827GR and H1975 cells had higher IC_{50} values for gefitinib compared with HCC827 cells (Fig. 2A). To confirm the correlation between TRIP13 expression and tolerance of NSCLC cells to gefitinib, the protein levels of TRIP13 in these cells were detected by western blotting. TRIP13 expression was significantly higher in HCC827GR and H1975 cells than in HCC827 cells (Fig. 2B and C). TRIP13 expression in NSCLC cells was upregulated or knocked down to determine the relationship between TRIP13 expression and gefitinib sensitivity. As revealed in Fig. 2, the IC_{50} of gefitinib was increased by upregulating the expression of TRIP13 in HCC827 cells (Fig. 2D) and decreased by the knockdown of TRIP13 in HCC827GR and H1975 cells (Fig. 2E and F), which verified our hypothesis that TRIP13 desensitizes NSCLC cells to gefitinib.

TRIP13 promotes the proliferation and colony formation while inhibiting the apoptosis of NSCLC cells in vitro. To further evaluate the role of TRIP13 in gefitinib sensitivity, the TRIP13 levels in cells (Fig. S2A and B) were adjusted and different

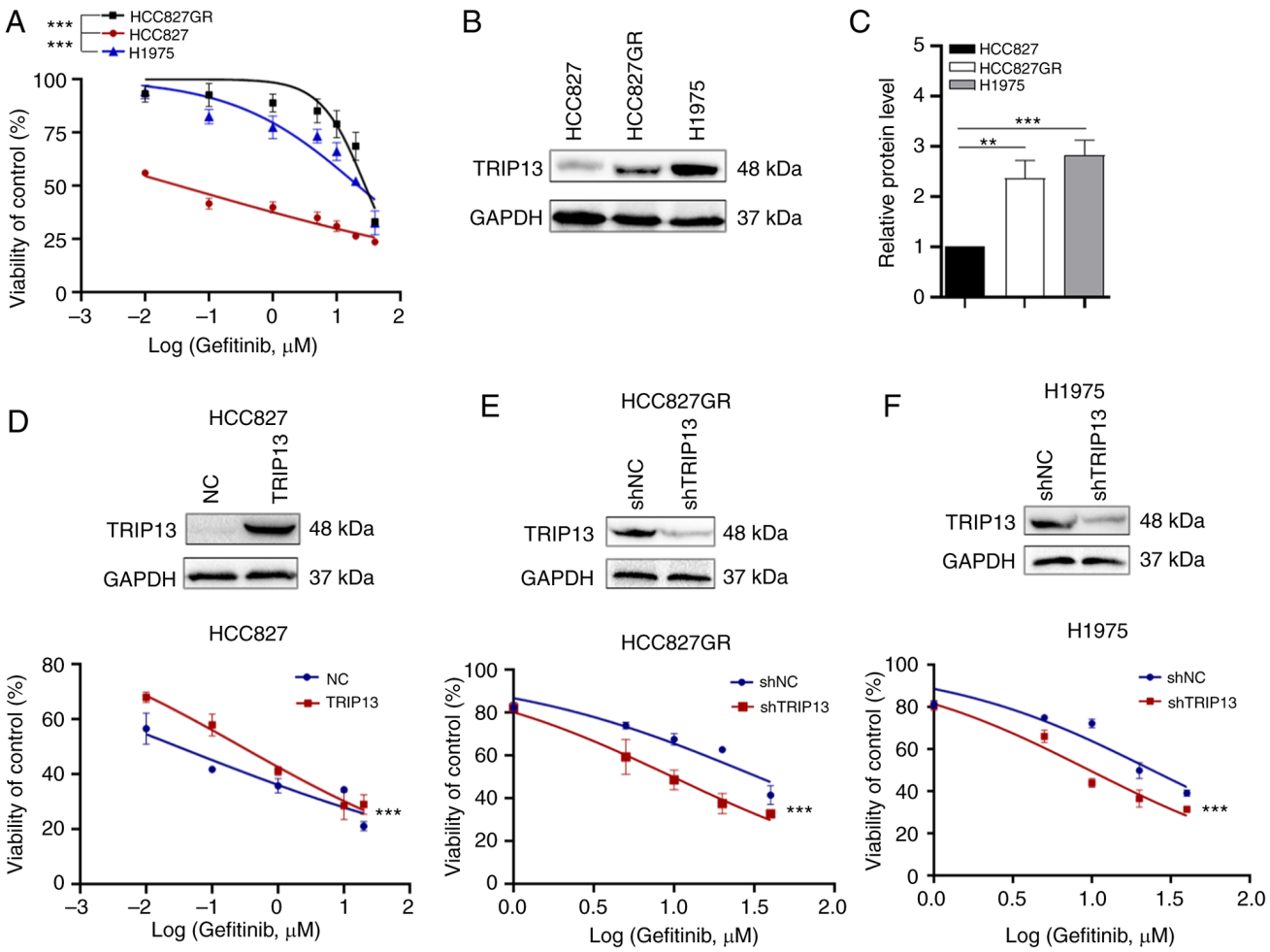

Figure 2. TRIP13 expression is elevated in gefitinib-resistant non-small cell lung cancer cells and inhibits gefitinib sensitivity. (A) Cell viability of HCC827, HCC827GR and H1975 cells treated with gefitinib. (B and C) TRIP13 protein expression and relative levels in HCC827, HCC827GR and H1975 cells. (D) Cell viability of HCC827 cells after gefitinib treatment combined with or without TRIP13 transfection. (E and F) Cell viability of HCC827GR and H1975 cells after gefitinib treatment combined with or without downregulation of TRIP13 expression. The data obtained were expressed as the mean ± SD. **P<0.01 and ***P<0.001. TRIP13, thyroid hormone receptor interactor 13; NC, negative control cells; sh-, short hairpin.

functional experiments related to drug resistance were performed. All NSCLC cells were treated with gefitinib to investigate whether TRIP13 induced drug resistance following gefitinib treatment. The results demonstrated that upregulation of TRIP13 expression enhanced the proliferation and colony formation of HCC827 cells (Fig. 3A and G), whereas downregulation of TRIP13 expression inhibited the proliferation and colony formation of HCC827GR (Fig. 3B and H) and H1975 (Fig. 3C and I) cells. Overexpression of TRIP13 decreased the apoptotic rate of HCC827 cells (Fig. 3D), whereas low TRIP13 expression increased the apoptosis of HCC827GR (Fig. 3E) and H1975 (Fig. 3F) cells.

TRIP13 promotes NSCLC cells proliferation in vivo. To evaluate the biological function of TRIP13 *in vivo*, HCC827 cells stably expressing TRIP13 and control HCC827 cells were subcutaneously injected into nude mice. The tumorigenic rates of the two groups were comparable (5/7, 71.4%), but the tumorigenic volume and weight were higher in the nude mice in the highly TRIP13-expressing group than in the control group (Fig. 4A-C). These findings indicated that TRIP13 plays a crucial regulatory role in fostering NSCLC cell proliferation *in vivo*.

TRIP13 contributes to autophagy in NSCLC cells. Immunocytochemical results identified that when TRIP13 was overexpressed in HCC827 cells, the number of LC3B-positive puncta (autophagosome-like structures) increased, indicating that autophagy was stimulated. Gefitinib acts as an autophagy agonist, improving the ability of TRIP13 to promote autophagy, while the autophagy inhibitor 3-MA diminished this effect (Fig. 5A and B). TRIP13 overexpression increased gefitinib-induced LC3B accumulation in HCC827 cells, whereas TRIP13 downregulation decreased gefitinib-induced LC3B accumulation in HCC827GR and H1975 cells. Meanwhile, 3-MA-induced P62 accumulation was enhanced by TRIP13 downregulation in HCC827GR and H1975 cells and reduced by TRIP13 upregulation in HCC827 cells (Fig. 5C-K).

TRIP13 interacts with EGFR in NSCLC cells. Given that EGFR plays a significant role in EGFR-TKI resistance, the function of TRIP13 in gefitinib resistance was further investigated by using the GEPIA database to predict the relationship between TRIP13 and EGFR. However, according to the database, TRIP13 expression did not correlate significantly with

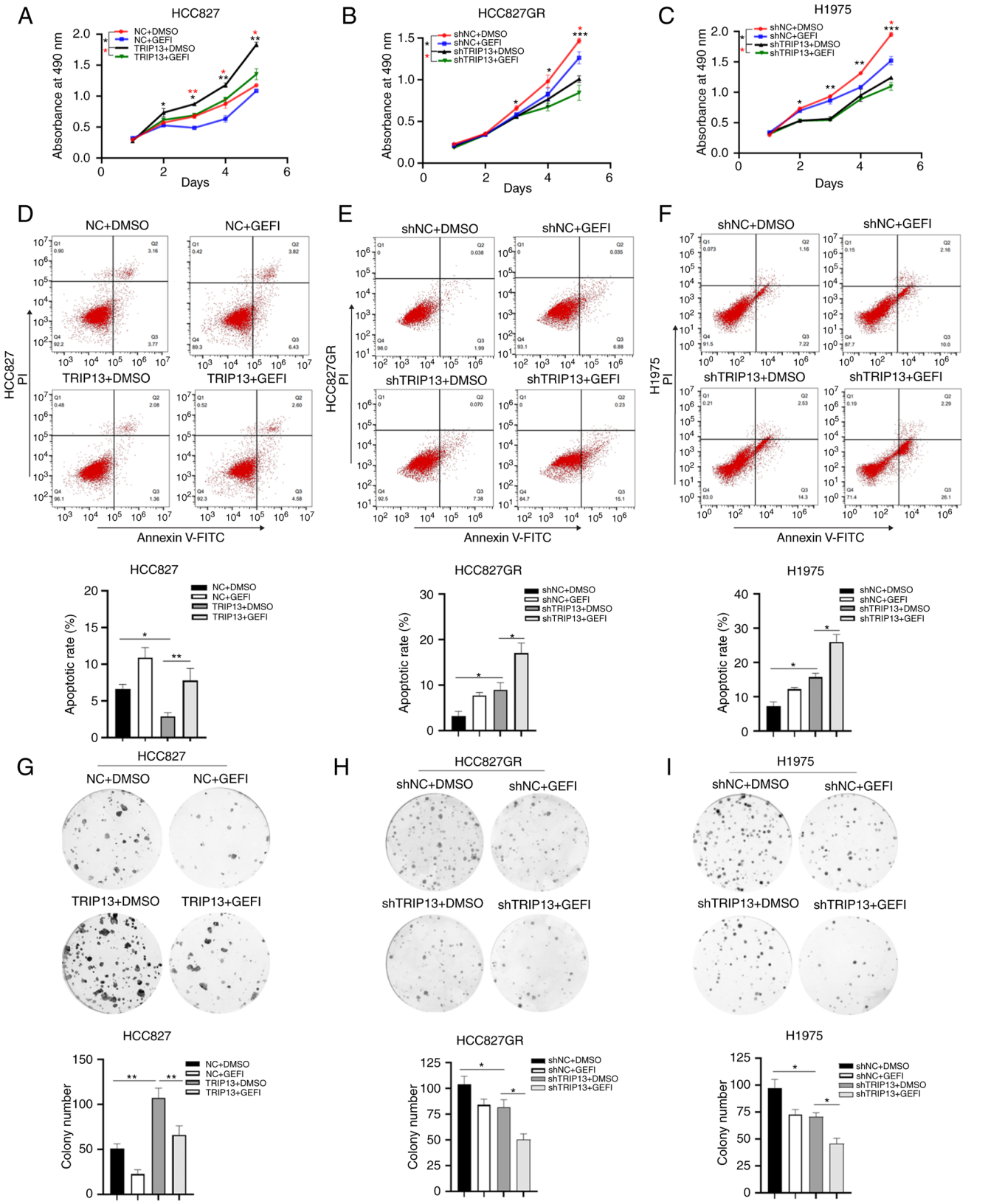

Figure 3. Effects of TRIP13 on the proliferation, colony formation and apoptosis of non-small cell lung cancer cells. (A) Growth curves of HCC827 cells with or without TRIP13 transfection and gefitinib treatment (0.5 μM). (B and C) Growth curves of HCC827GR and H1975 cells with or without downregulation of TRIP13 and gefitinib treatment (5 μM). (D-I) Images and histograms of (D-F) cell apoptosis and (G-I) colony formation assays in HCC827, HCC827GR and H1975 cells treated as indicated. The data obtained were expressed as the mean ± SD. *P<0.05, **P<0.01 and ***P<0.001. TRIP13, thyroid hormone receptor interactor 13; GEFI, gefitinib; DMSO, dimethyl sulfoxide (used as a negative control for the cells); NC, negative control cells; sh-, short hairpin.

EGFR expression in NSCLC cells (Fig. 6A-C). Using laser confocal immunofluorescence, it was observed that TRIP13 and EGFR were primarily colocalized in the cytoplasm of NSCLC cells (Fig. 6D). Finally, co-immunoprecipitation

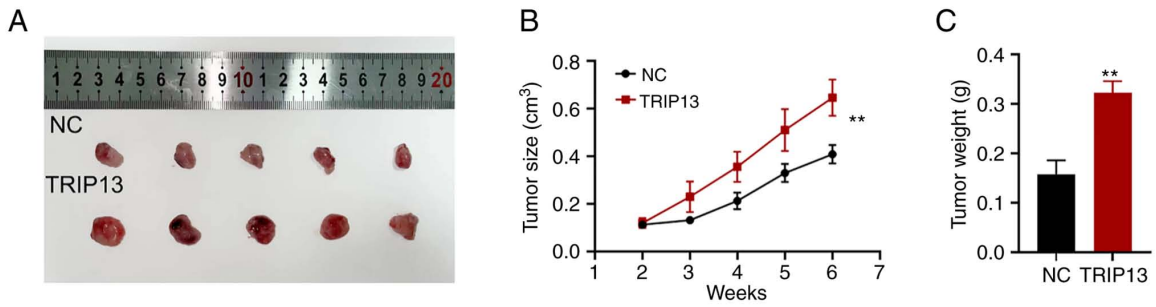

Figure 4. Effect of TRIP13 expression on the proliferation in xenograft mouse models. (A) Subcutaneous injection of HCC827 cells with stable expression of TRIP13 (screened by G418) into nude mice. HCC827 cells transfected with empty vector served as control cells. (B) The average tumor volume of two groups of nude mice. (C) The average tumor weight of two groups of nude mice. The data obtained were expressed as the mean ± SD. **P<0.01. TRIP13, thyroid hormone receptor interactor 13; NC, negative control cells.

experiments confirmed that TRIP13 could bind to EGFR in both gefitinib-sensitive and gefitinib-resistant NSCLC cells (Fig. 6E).

TRIP13 activates the phosphorylation of EGFR and its downstream signaling pathways in NSCLC cells. TRIP13 was discovered to activate the PI3K/AKT/mTOR signaling pathway in lung cancers, which was likewise in line with the data from TCGA database (Fig. S2C). However, the relationship between TRIP13 and the EGFR pathway in lung cancer has not been clarified. To further study the effect of TRIP13 on EGFR, it was examined whether the EGFR inhibitor gefitinib affected TRIP13 expression in the three cell lines. According to the results of western blotting, TRIP13 expression decreased with increasing gefitinib concentration (Fig. 7A-C). The expression levels of TRIP13 were then changed in HCC827, HCC827GR and H1975 cells and the alterations in the total and phosphorylated (p-)EGFR (Tyr1068) at the protein level were examined. P-EGFR (Tyr1068) levels were increased along with TRIP13 overexpression in HCC827 cells and decreased after TRIP13 downregulation in HCC827GR and H1975 cells. TRIP13 upregulation also enhanced total EGFR levels in HCC827 cells, whereas TRIP13 knockdown reduced its levels in HCC827GR and H1975 cells. Notably, the level of p-EGFR was significantly altered compared with that of total EGFR. Alterations in downstream phosphorylated key proteins of the EGFR pathway, including p-JAK (Tyr1007 and Tyr1008), p-STAT3 (Tyr705), p-PI3K (Tyr 199), p-AKT (Ser473), p-MEK (Ser217 and Ser221) and p-ERK (Thr202 and Tyr187), were consistent with those of p-EGFR (Tyr1068). However, despite changes in the expression of TRIP13, the total protein levels of the abovementioned downstream proteins were not significantly altered. As an EGFR inhibitor, gefitinib reversed the effects of TRIP13 on EGFR and its downstream proteins (Fig. 7D-G).

Discussion

In lung cancer, TRIP13 has been found to promote carcinogenesis by activating the PI3K/AKT/mTOR signaling pathway, which is also consistent with the TCGA data. However, the underlying mechanisms remain unknown (17,18). The role of TRIP13 in tumor drug resistance has markedly received attention in recent years. TRIP13 induces cisplatin and doxorubicin resistance in bladder cancer cells and desensitizes head and neck cancers to radiation and cetuximab. In addition, TRIP13 molecular inhibitors have a beneficial synergistic effect against multiple myeloma (20-22). However, the relationship between TRIP13 and gefitinib resistance in NSCLC has not been reported.

In the present study, HCC827 (with *EGFR* 19del) and H1975 (with *EGFR* L858R and T790M mutations) cells were used as gefitinib-sensitive and gefitinib-resistant NSCLC cells, respectively. HCC827GR cells were used to investigate the role of TRIP13 in the development of gefitinib resistance in NSCLC. TRIP13 expression was higher in gefitinib-resistant cells than in gefitinib-sensitive cells. It was hypothesized that both *EGFR* T790M mutation and continuous gefitinib treatment would increase TRIP13 expression, leading to the development of a gefitinib-resistant phenotype. Alterations in the IC_{50} values of NSCLC cells were correlated with changes in TRIP13 protein levels. As revealed by colony formation, proliferation and apoptosis assays *in vitro*, TRIP13 overexpression lowered the susceptibility of HCC827 cells to gefitinib, whereas TRIP13 knockdown restored gefitinib sensitivity in both H1975 and HCC827GR cells. A possible explanation for the aforementioned results is that TRIP13 expression was enhanced in gefitinib-resistant cells compared with that in gefitinib-sensitive cells, promoting cell proliferation and colony formation and inhibiting apoptosis, ultimately leading to gefitinib resistance. Taken together, the aforementioned findings indicated that TRIP13 plays a critical role in gefitinib resistance and suggested that TRIP13 may be a potential biomarker for gefitinib resistance in NSCLC.

Considering that patients with advanced lung cancer develop TKI-induced autophagy following long-term gefitinib treatment and that autophagy promotes gefitinib resistance (34,35), the relationship between TRIP13 and autophagy was investigated using DMSO as a control, gefitinib as an autophagy agonist and 3-MA as an autophagy inhibitor. Immunofluorescence results suggested that TRIP13 increased the number of LC3B-positive puncta in the NSCLC cells. Moreover, TRIP13 overexpression increased LC3B and decreased P62 expression levels in HCC827 cells. TRIP13 downregulation had the opposite effects in H1975 and HCC827GR cells. All aforementioned effects were improved by gefitinib treatment and reversed by 3-MA. Therefore, TRIP13 may induce gefitinib resistance in NSCLC cells

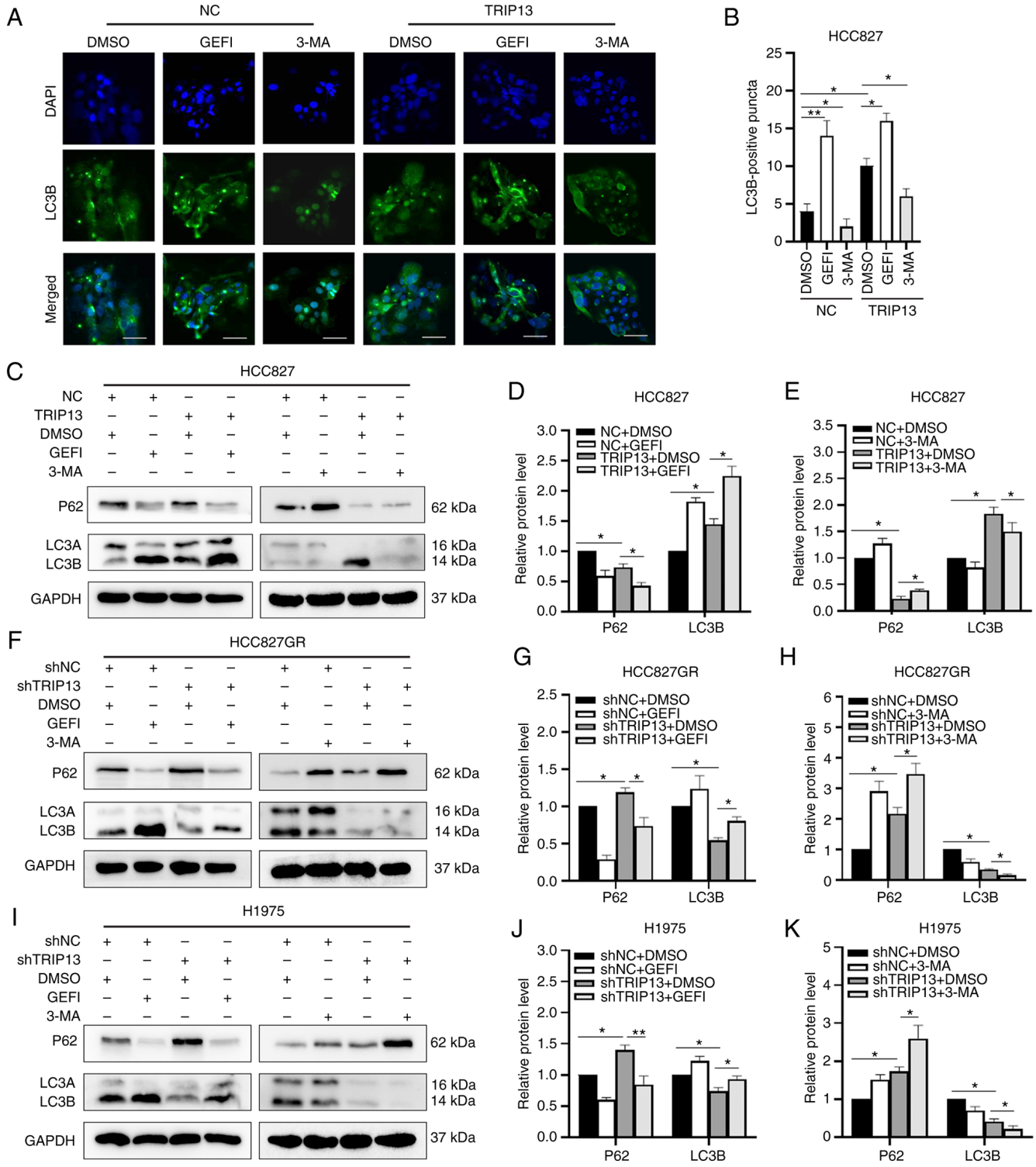

Figure 5. Effect of TRIP13 on autophagy of non-small cell lung cancer cells. (A) Representative immunofluorescence images of HCC827 cells with or without TRIP13 upregulation following treatment with gefitinib (0.5 μM for 12 h) or 3-MA (10 mM for 12 h). Scale bar, 10 μm. (B) Numbers of LC3B-positive puncta (autophagosome-like structures) in HCC827 cells with or without TRIP13 upregulation. A total of 20 cells were counted from every independent experiment, which was repeated thrice and calculated. (C) Expression levels of LC3 and P62 proteins in HCC827 cells following TRIP13 overexpression and treatment with gefitinib (0.5 μM for 12 h, left) or 3-MA (10 mM for 12 h, right). (F and I) LC3 and P62 protein expression levels in H1975 and HCC827GR cells after TRIP13 knockdown and treatment with gefitinib (5 μM for 12 h, left) or 3-MA (10 mM for 12 h, right). (D, E, G, H, J and K) Relative expression levels of proteins for each group are displayed in the histograms. DMSO and GAPDH were used as drug control and internal control, respectively. The data obtained were expressed as the mean ± SD. *P<0.05 and **P<0.01. TRIP13, thyroid hormone receptor interactor 13; LC3A, microtubule-associated protein 1 light chain 3 alpha; LC3B, microtubule-associated protein 1 light chain 3 beta; P62, also known as SQSTM1, Sequestosome 1; DMSO, dimethyl sulfoxide; GEFI, gefitinib; 3-MA, 3-Methyladenine; NC, negative control cells; sh-, short hairpin.

by enhancing autophagy. Notably, TRIP13 promoted lung carcinogenesis by triggering the PI3K/AKT/mTOR pathway. However, the activation of this pathway suppresses autophagy, which contradicts the findings of the present findings (36).

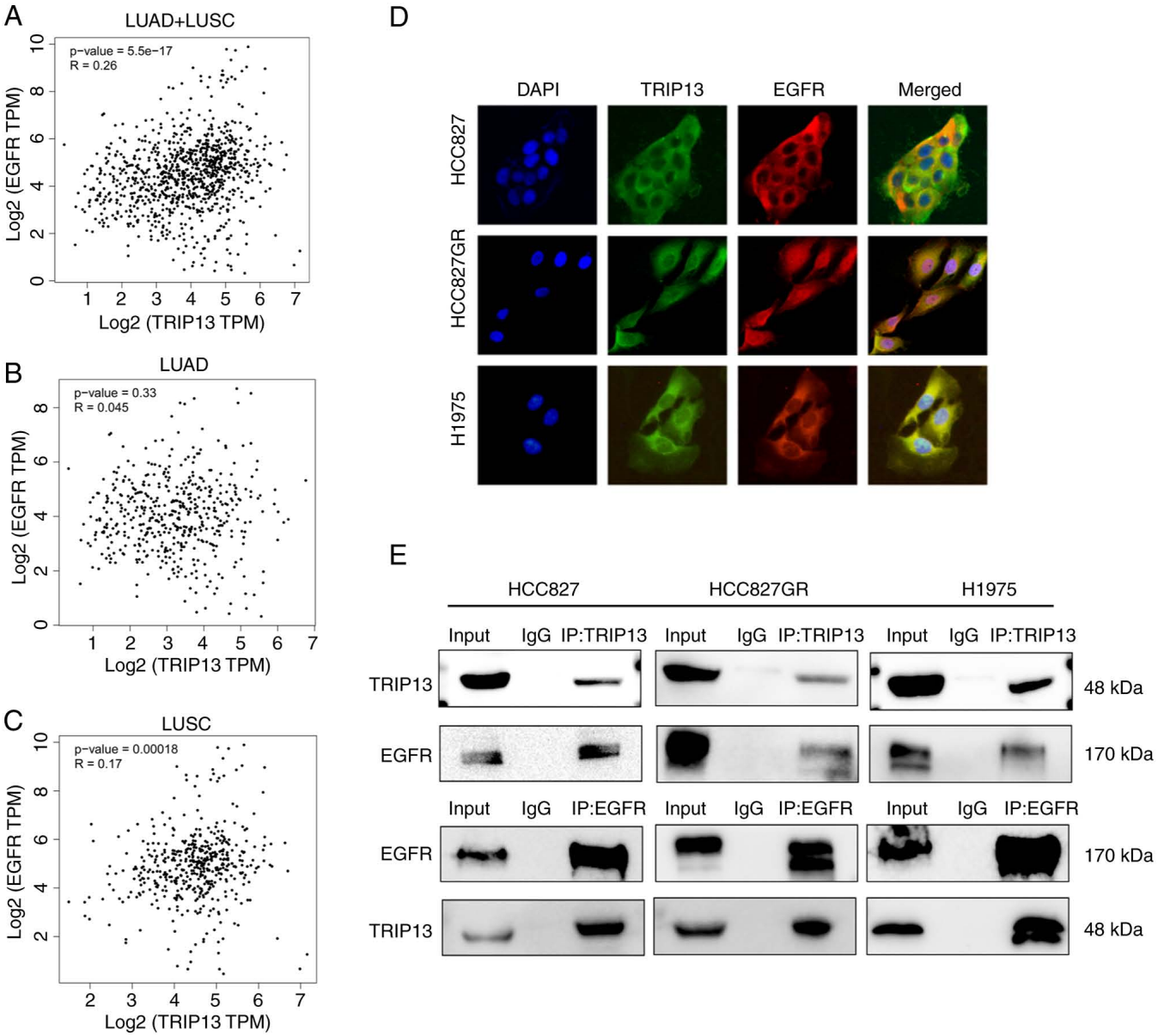

Figure 6. Localization and interaction of TRIP13 with EGFR in non-small cell lung cancer cells. (A-C) Correlation scatter plots of TRIP13 and EGFR expression levels in LUAD and LUSC. Data were obtained from the Gene Expression Profiling Interactive Analysis database. (D) Laser confocal immunofluorescence analysis showed that TRIP13 and EGFR mainly co-localized in the cytoplasm of HCC827, H1975 and HCC827GR cells (magnification, x400). DAPI was used to stain cell nuclei. (E) Co-immunoprecipitation analysis of the interaction between TRIP13 and EGFR in HCC827, H1975 and HCC827GR cells. TRIP13, thyroid hormone receptor interactor 13; EGFR, epidermal growth factor receptor; LUAD, lung adenocarcinoma; LUSC, lung squamous cell carcinoma.

The authors' hypothesis concerning this contradiction was that TRIP13 overexpression inhibited autophagy by triggering the PI3K/AKT/mTOR pathway. It also enhanced autophagy via other pathways, such as promoting drug resistance-related pathways or directly regulating key autophagy-related proteins, which had a greater impact on improving autophagy than the PI3K/AKT/mTOR pathway. TRIP13 generally promotes autophagy.

Although the GEPIA database did not demonstrate a significant correlation between TRIP13 and EGFR in NSCLC cells, immunofluorescence and co-immunoprecipitation assays confirmed that TRIP13 colocalized with EGFR in the cytoplasm and underwent protein interactions in NSCLC cells. Notably, EGFR was found in both the cell membrane and cytoplasm of HCC827 cells but was mostly located in the nucleus and less in the cytoplasm of HCC827GR cells. Long-term gefitinib therapy in sensitive cells resulted in a shift in EGFR location from the cytoplasm to the nucleus. Indeed, the change in EGFR location in cells is also one of the reasons why EGFR-TKI resistance arises, as demonstrated in a previous study (37). There is a positive protein interaction between TRIP13 and EGFR, thus the expression of TRIP13 will decrease along with EGFR after gefitinib is added. When EGFR interacts with ligands, it activates various downstream signaling pathways via phosphorylation. The main pathways implicated in EGFR-TKI resistance include the MEK/ERK, JAK/STAT3 and PI3K/Akt/mTOR signaling pathways. All three pathways are downstream of EGFR and have been implicated in several malignancies (29-32). In contrast to the PI3K/AKT/mTOR pathway, which suppresses

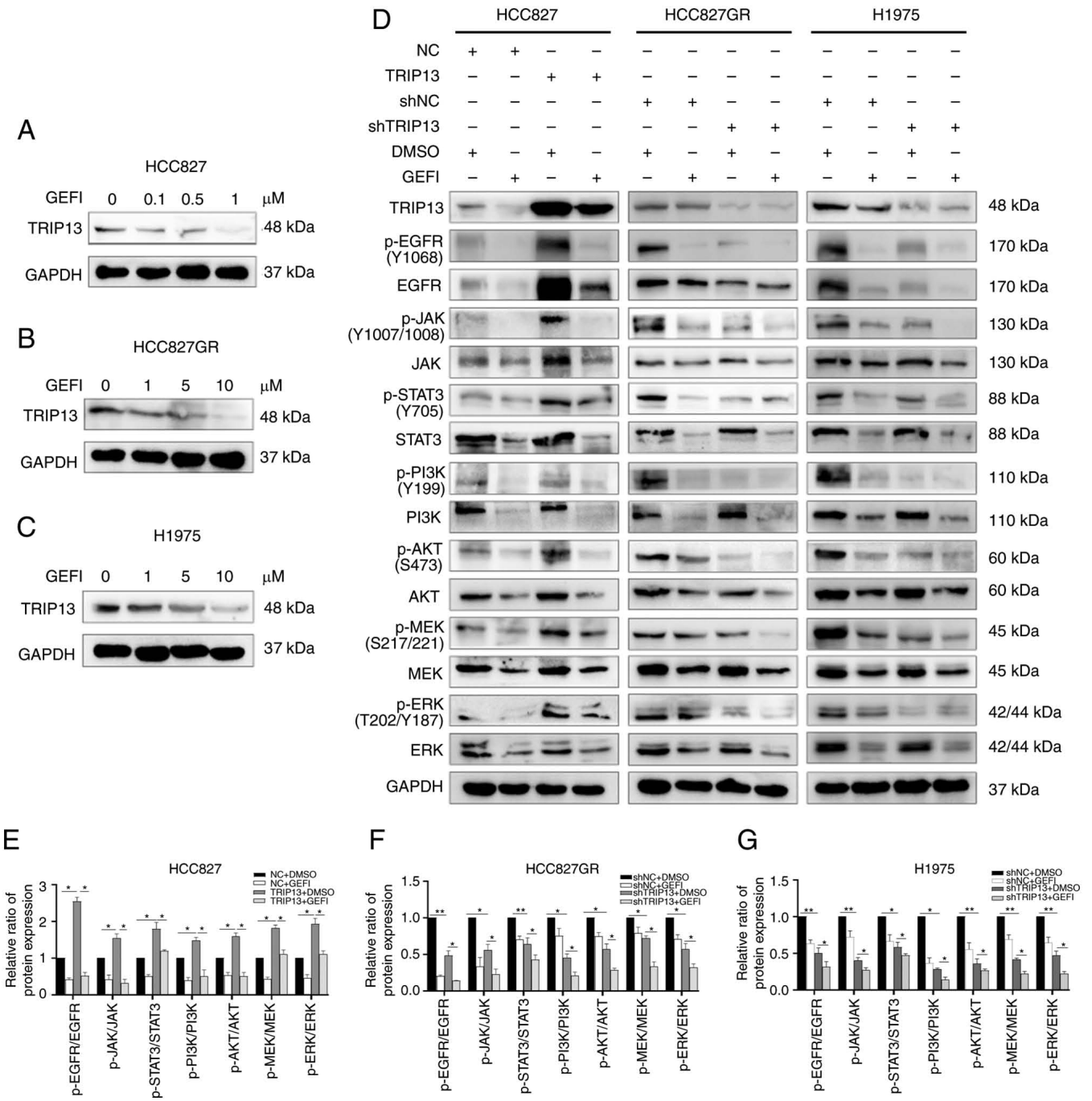

Figure 7. TRIP13 increases the expression of key EGFR pathway proteins in NSCLC cells. (A-C) Western blot analysis showing the dose-dependent decrease of TRIP13 levels induced by gefitinib at 12 h in HCC827, HCC827GR and H1975 NSCLC cells. (D) Expression of key EGFR pathway proteins in HCC827 (treated with 0.5 μM gefitinib for 12 h), H1975 and HCC827GR cells (treated with 5 μM gefitinib for 12 h) after TRIP13 overexpression or knockdown. (E-G) Relative expression levels of proteins for each group determined via western blotting. DMSO and GAPDH were used as drug control and internal control, respectively. The data obtained were expressed as the mean ± SD. *P<0.05 and **P<0.01. TRIP13, thyroid hormone receptor interactor 13; EGFR, epidermal growth factor receptor; NSCLC, non-small cell lung cancer; EGFR, epidermal growth factor receptor (Tyr1068); JAK, Janus kinase (Tyr1007/1008); STAT3, signal transducer and activator of transcription 3 (Tyr705); PI3K, phosphatidylinositol-4,5-bisphosphate 3-kinase (Tyr199); AKT, V-akt murine thymoma viral oncogene homolog (Ser473); MEK, mitogen-activated protein kinase (Ser217/221); ERK, mitogen-activated protein kinase (Thr202/Tyr187); DMSO, dimethyl sulfoxide; GEFI, gefitinib; p-, phosphorylated; NC, negative control cells; sh-, short hairpin.

autophagy, both the MEK/ERK and JAK/STAT3 pathways increase autophagy. It was identified that TRIP13 upregulation enhanced the protein phosphorylation levels of EGFR downstream pathways, whereas TRIP13 downregulation had the opposite effect. TRIP13 contributes to the phosphorylation of the EGFR signaling pathway in NSCLC, resulting in gefitinib resistance.

However, the present study has not examined the expression alterations of TRIP13 in NSCLC patients before and after gefitinib treatment, and patients with gefitinib-resistant, which will help to confirm the present results. The specific mechanism by which TRIP13 induces autophagy and gefitinib resistance in NSCLC remains unclear. The specific role of TRIP13 in second- and third-generation TKIs including afatinib and

osimertinib also needs to be confirmed. In addition, it is crucial to determine whether TRIP13 is involved in pathways other than EGFR for gefitinib resistance in NSCLC. Further studies are needed to understand the mechanisms underlying this phenomenon and confirm the therapeutic applicability of these drugs.

In conclusion, the present study indicated that TRIP13 could induce gefitinib resistance in NSCLC by promoting autophagy and phosphorylation of the EGFR signaling pathway. Thus, TRIP13 can be used as a biomarker and therapeutic target for gefitinib-resistant NSCLC.

Acknowledgements

Not applicable.

Funding

The present study was supported by the Natural Science Foundation of Liaoning (grant no. 2020-MS-179).

Availability of data and materials

The datasets used and analyzed during the current study are available from the corresponding author on reasonable request.

Authors' contributions

ZXX designed the study, carried out the experiments, collected and analyzed the data and wrote the manuscript. MXL and XQZ made recommendations and helped with data analysis. XZR and HTX were in charge of the conception and supervision of the study. All authors revised draft versions and read and approved the final manuscript. ZXX and HTX confirm the authenticity of all the raw data.

Ethics approval and consent to participate

The present study was approved [approval no. LS (2021)009] by the Research Ethics Committee of the China Medical University. The animal research protocol was reviewed and approved (IACUC Issue no. KT2022488) by the Institutional Animal Research Committee of China Medical University (Shenyang, China). Written informed consent was obtained from all patients.

Patient consent for publication

Not applicable.

Competing interests

The authors declare that they have no competing interests.

References

1. Siegel RL, Miller KD, Fuchs HE and Jemal A: Cancer statistics, 2021. CA Cancer J Clin 71: 7-33, 2021.
2. Shigematsu H, Lin L, Takahashi T, Nomura M, Suzuki M, Wistuba II, Fong KM, Lee H, Toyooka S, Shimizu N, *et al*: Clinical and biological features associated with epidermal growth factor receptor gene mutations in lung cancers. J Natl Cancer Inst 97: 339-346, 2005.
3. Majem M and Remon J: Tumor heterogeneity: Evolution through space and time in EGFR mutant non small cell lung cancer patients. Transl Lung Cancer Res 2: 226-237, 2013.
4. Westover D, Zugazagoitia J, Cho BC, Lovly CM and Paz-Ares L: Mechanisms of acquired resistance to first- and second-generation EGFR tyrosine kinase inhibitors. Ann Oncol 29 (suppl_1): i10-i19, 2018.
5. Clairmont CS, Sarangi P, Ponnienselvan K, Galli LD, Csete I, Moreau L, Adelmant G, Chowdhury D, Marto JA and D'Andrea AD: TRIP13 regulates DNA repair pathway choice through REV7 conformational change. Nat Cell Biol 22: 87-96, 2020.
6. Ma HT and Poon RY: TRIP13 functions in the establishment of the spindle assembly checkpoint by replenishing O-MAD2. Cell Rep 22: 1439-1450, 2018.
7. Ye Q, Kim DH, Dereli I, Rosenberg SC, Hagemann G, Herzog F, Tóth A, Cleveland DW and Corbett KD: The AAA+ ATPase TRIP13 remodels HORMA domains through N-terminal engagement and unfolding. EMBO J 36: 2419-2434, 2017.
8. Alfieri C, Chang L and Barford D: Mechanism for remodelling of the cell cycle checkpoint protein MAD2 by the ATPase TRIP13. Nature 559: 274-278, 2018.
9. Yost S, de Wolf B, Hanks S, Zachariou A, Marcozzi C, Clarke M, de Voer R, Etemad B, Uijttewaal E, Ramsay E, *et al*: Biallelic TRIP13 mutations predispose to Wilms tumor and chromosome missegregation. Nat Genet 49: 1148-1151, 2017.
10. Raina VB and Vader G: Homeostatic control of meiotic prophase checkpoint function by Pch2 and Hop1. Curr Biol 30: 4413-4424. e5, 2020.
11. Li C, Xia J, Franqui-Machin R, Chen F, He Y, Ashby TC, Teng F, Xu H, Liu D, Gai D, *et al*: TRIP13 modulates protein deubiquitination and accelerates tumor development and progression of B cell malignancies. J Clin Invest 131: e146893, 2021.
12. Sheng N, Yan L, Wu K, You W, Gong J, Hu L, Tan G, Chen H and Wang Z: TRIP13 promotes tumor growth and is associated with poor prognosis in colorectal cancer. Cell Death Dis 9: 402, 2018.
13. Zhang G, Zhu Q, Fu G, Hou J, Hu X, Cao J, Peng W, Wang X, Chen F and Cui H: TRIP13 promotes the cell proliferation, migration and invasion of glioblastoma through the FBXW7/c-MYC axis. Br J Cancer 121: 1069-1078, 2019.
14. Zhou XY and Shu XM: TRIP13 promotes proliferation and invasion of epithelial ovarian cancer cells through notch signaling pathway. Eur Rev Med Pharmacol Sci 23: 522-529, 2019.
15. Dong L, Ding H, Li Y, Xue D, Li Z, Liu Y, Zhang T, Zhou J and Wang P: TRIP13 is a predictor for poor prognosis and regulates cell proliferation, migration and invasion in prostate cancer. Int J Biol Macromol 121: 200-206, 2019.
16. Yu L, Xiao Y, Zhou X, Wang J, Chen S, Peng T and Zhu X: TRIP13 interference inhibits the proliferation and metastasis of thyroid cancer cells through regulating TTC5/p53 pathway and epithelial-mesenchymal transition related genes expression. Biomed Pharmacother 120: 109508, 2019.
17. Cai W, Ni W, Jin Y and Li Y: TRIP13 promotes lung cancer cell growth and metastasis through AKT/mTORC1/c-Myc signaling. Cancer Biomark 30: 237-248, 2021.
18. Li W, Zhang G, Li X, Wang X, Li Q, Hong L, Shen Y, Zhao C, Gong X, Chen Y and Zhou J: Thyroid hormone receptor interactor 13 (TRIP13) overexpression associated with tumor progression and poor prognosis in lung adenocarcinoma. Biochem Biophys Res Commun 499: 416-424, 2018.
19. Li ZH, Lei L, Fei LR, Huang WJ, Zheng YW, Yang MQ, Wang Z, Liu CC and Xu HT: TRIP13 promotes the proliferation and invasion of lung cancer cells via the Wnt signaling pathway and epithelial-mesenchymal transition. J Mol Histol 52: 11-20, 2021.
20. Wang Y, Huang J, Li B, Xue H, Tricot G, Hu L, Xu Z, Sun X, Chang S, Gao L, *et al*: A small-molecule inhibitor targeting TRIP13 suppresses multiple myeloma progression. Cancer Res 80: 536-548, 2020.
21. Banerjee R, Liu M, Bellile E, Schmitd LB, Goto M, Hutchinson MN, Singh P, Zhang S, Damodaran DP, Nyati MK, *et al*: Phosphorylation of TRIP13 at Y56 induces radiation resistance but sensitizes head and neck cancer to cetuximab. Mol Ther 30: 468-484, 2022.
22. Lu S, Guo M, Fan Z, Chen Y, Shi X, Gu C and Yang Y: Elevated TRIP13 drives cell proliferation and drug resistance in bladder cancer. Am J Transl Res 11: 4397-4410, 2019.
23. Levine B and Kroemer G: Biological functions of autophagy genes: A disease perspective. Cell 176: 11-42, 2019.

24. Galluzzi L and Green DR: Autophagy-independent functions of the autophagy machinery. Cell 177: 1682-1699, 2019.
25. Dikic I and Elazar Z: Mechanism and medical implications of mammalian autophagy. Nat Rev Mol Cell Biol 19: 349-364, 2018.
26. Wu M and Zhang P: EGFR-mediated autophagy in tumourigenesis and therapeutic resistance. Cancer Lett 469: 207-216, 2020.
27. Li YJ, Lei YH, Yao N, Wang CR, Hu N, Ye WC, Zhang DM and Chen ZS: Autophagy and multidrug resistance in cancer. Chin J Cancer 36: 52, 2017.
28. Amaravadi RK, Kimmelman AC and Debnath J: Targeting autophagy in cancer: Recent advances and future directions. Cancer Discov 9: 1167-81, 2019.
29. Sigismund S, Avanzato D and Lanzetti L: Emerging functions of the EGFR in cancer. Mol Oncol 12: 3-20, 2018.
30. Cheng WL, Feng PH, Lee KY, Chen KY, Sun WL, Van Hiep N, Luo CS and Wu SM: The role of EREG/EGFR pathway in tumor progression. Int J Mol Sci 22: 12828, 2021.
31. Pao W and Miller VA: Epidermal growth factor receptor mutations, small-molecule kinase inhibitors, and non-small-cell lung cancer: Current knowledge and future directions. J Clin Oncol 23: 2556-2568, 2005.
32. Liu Q, Yu S, Zhao W, Qin S, Chu Q and Wu K: EGFR-TKIs resistance via EGFR-independent signaling pathways. Mol Cancer 17: 53, 2018.
33. Bradford MM: A rapid and sensitive method for the quantitation of microgram quantities of protein utilizing the principle of protein-dye binding. Anal Biochem 72: 248-254, 1976.
34. Han W, Pan H, Chen Y, Sun J, Wang Y, Li J, Ge W, Feng L, Lin X, Wang X, *et al*: EGFR tyrosine kinase inhibitors activate autophagy as a cytoprotective response in human lung cancer cells. PLoS One 6: e18691, 2011.
35. Li YY, Lam SK, Mak JC, Zheng CY and Ho JC: Erlotinib-induced autophagy in epidermal growth factor receptor mutated non-small cell lung cancer. Lung Cancer 81: 354-361, 2013.
36. Gremke N, Polo P, Dort A, Schneikert J, Elmshäuser S, Brehm C, Klingmüller U, Schmitt A, Reinhardt HC, Timofeev O, *et al*: mTOR-mediated cancer drug resistance suppresses autophagy and generates a druggable metabolic vulnerability. Nat Commun 11: 4684, 2020.
37. Rong X, Liang Y, Han Q, Zhao Y, Jiang G, Zhang X, Lin X, Liu Y, Zhang Y, Han X, *et al*: Molecular mechanisms of tyrosine kinase inhibitor resistance induced by membranous/cytoplasmic/nuclear translocation of epidermal growth factor receptor. J Thorac Oncol 14: 1766-1783, 2019.